

Structural study of the ferroelectric phase transition of vinylidene fluoride–trifluoroethylene copolymers: 4. Poling effect on structure and phase transition

Kohji Tashiro and Masamichi Kobayashi

Department of Macromolecular Science, Faculty of Science, Osaka University, Toyonaka, Osaka 560, Japan

(Received 12 April 1985; revised 17 May 1985)

A structural change induced by poling has been investigated for vinylidene fluoride–trifluoroethylene (VDF–TrFE) copolymers with VDF molar contents of 52% and 65% using the X-ray diffraction and infra-red spectroscopic methods. Before poling, the crystalline phase of these copolymers is in a disordered state with essentially *trans* zigzag chains tilted slightly from the draw direction (the so-called cooled phase). After poling under a high d.c. voltage, these samples transfer to the more regular ferroelectric 'low-temperature' phase. Just then the dipoles of the *trans* chains orient into the direction of the applied electric field with the tilting angle unchanged or with the tilted segments reoriented vertically along the draw direction. Following such a structural change, the phase transitional behaviour has also been found to be affected greatly by the poling treatment. After poling, the transition point from the ferroelectric *trans* phase to the paraelectric *gauche* phase shifts by about 10°C to the higher-temperature side and the transition itself becomes much sharper.

(Keywords: vinylidene fluoride–trifluoroethylene copolymers; poling treatment; crystal structures; ferroelectric phase transition)

INTRODUCTION

In previous papers^{1–5} we analysed the crystal and molecular structural change occurring in the ferroelectric–paraelectric phase transition of vinylidene fluoride–trifluoroethylene (VDF–TrFE) copolymers and clarified several important factors governing the transitional behaviour. The transitional behaviour changes greatly from sample to sample with different VDF molar content. For example, in the case of copolymer with 55% VDF molar content (abbreviated as VDF 55% copolymer), there exist three kinds of crystal phases as shown in *Figure 1*. The ferroelectric low-temperature phase consists of polar unit cells where the zigzag chains are packed so that the dipoles are parallel along the *b* axis. The structure is essentially the same as that of PVDF form I⁶. When this low-temperature phase is heated above the transition temperature of about 65°C, it transfers into the high-temperature paraelectric phase (via the cooled phase²), where the molecular chains are constructed by a statistical combination of *TT*, *TG* and *TG* rotational isomers (*T* = *trans*, *G* = *gauche*) and rotate violently around the chain axis so that the unit cell is nonpolar. On cooling down to room temperature, the high-temperature phase does not go back to the original low-temperature phase but transfers into the so-called 'cooled phase'. Based on X-ray diffraction and infra-red and Raman spectroscopy, we propose a possible structure model of this phase shown in *Figure 1*; the cooled phase has a kind of superlattice structure consisting of an aggregation of polar domains. Each domain is constructed by a parallel arrangement of all-*trans* zigzag

chains and the unit cell structure is almost equivalent to that of the low-temperature phase and PVDF form I. The *trans* segments in these domains are linked together by *skew* or equivalent *trans-gauche* linkages along the chain axis, resulting in a tilting of the segments by about 18° from the draw direction in the (130) plane. This is observed in a form of tilting phenomenon of X-ray reflections⁷. The dipole moments of the neighbouring *trans* segments connected by *skew* (or *trans-gauche*) linkages make an angle 60° to each other, leading naturally to the so-called 60° domain, where the polar axis of each domain points in the direction of 0° or ±60° from the standard *b* axis by a statistical weight of 1/3. Such a characteristic structure gives a minimal *R* factor for X-ray diffraction intensities. Spatial fitting of the neighbouring domains is not necessarily so good, and therefore the cooled phase is in a considerably disordered state as understood from the broad and diffuse X-ray scattering pattern.

When the cooled phase is tensioned strongly along the draw axis at room temperature, it transforms into the highly regular crystal structure of the low-temperature ferroelectric phase². The tensile force may induce the conformational change of the above-mentioned linking parts from *skew* (*gauche*) to *trans*. Then the tilting of *trans* segments and the 60° domain structure disappear simultaneously, resulting in a single-domain-like structure of nontilted all-*trans* chains. Such an ordering in crystal structure is also induced by the application of high electric field on the cooled phase, as pointed out by Lovinger *et al.*^{8–11}. But we can expect that the crystal

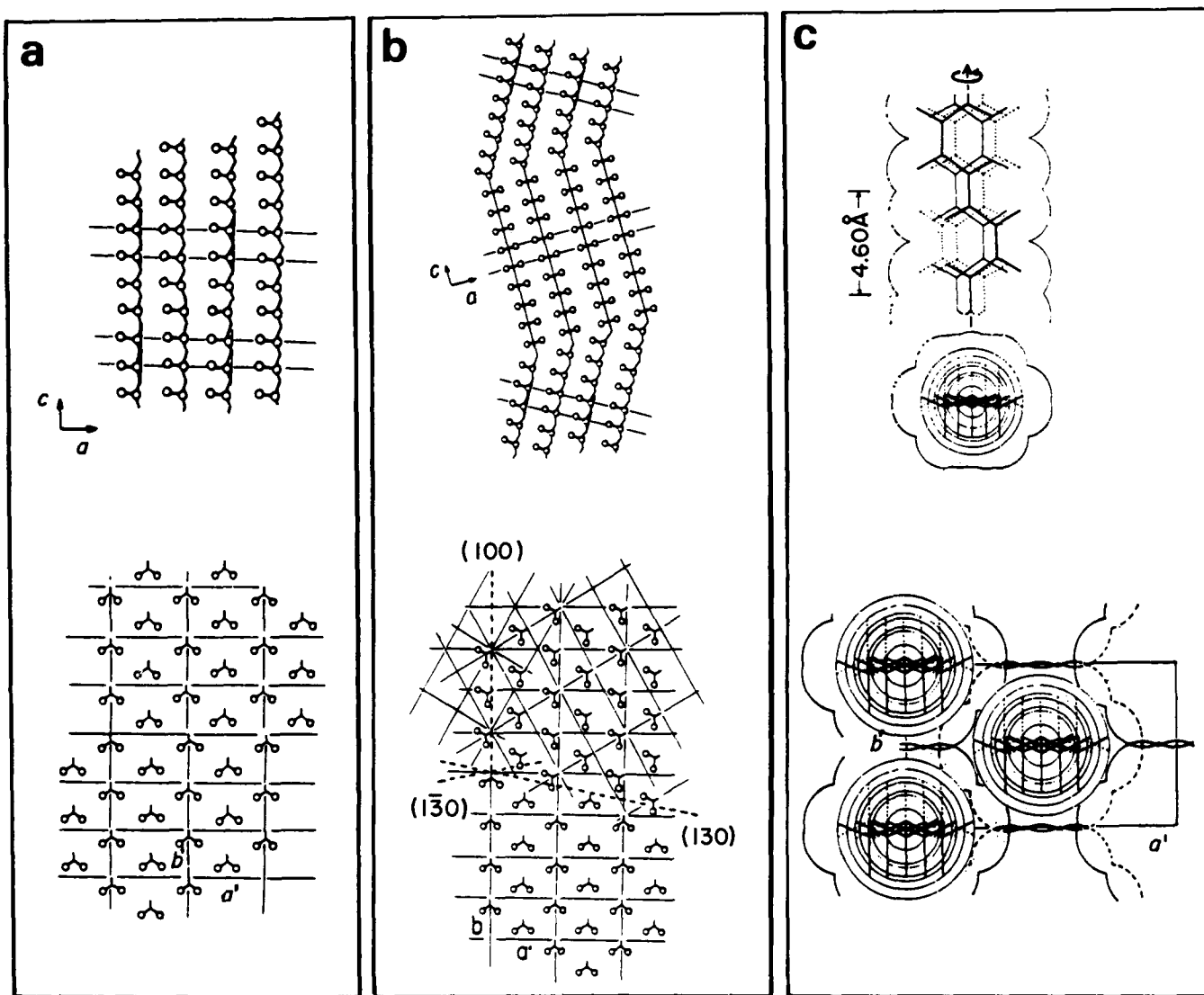


Figure 1 Crystal structure models of (a) the low-temperature phase, (b) the cooled phase and (c) the high-temperature phase of VDF 55% copolymer^{2,3}

structure thus obtained might be different from that obtained by the tensile stress, because, for the oriented sample, the electric field is applied to the film surface or perpendicularly to the draw direction while the tensile force works along the draw axis. In this paper we will report effects of externally applied electric and mechanical fields on the crystal structure and transitional behaviour of copolymers by X-ray diffraction and infra-red spectroscopic methods.

EXPERIMENTAL

Samples

The samples used were VDF-TrFE random copolymers with VDF molar contents of 52% and 65%, supplied by Diakin Kogyo Co. Ltd (Japan). The oriented films were prepared by elongating the melt-quenched sample by about five times the original length at room temperature and then heat-treating at about 120°C for 3 h. The samples thus obtained are of the cooled phase. The samples were corona-charged at room temperature for about 30 min using a pin (positive) and plate (negative) electrode system (an inter-electrode distance of about 1 cm) with a high d.c. voltage of about 10 kV.

Measurements

X-ray photographs were taken with cylindrical and Weissenberg cameras. The temperature dependence of the X-ray diffraction pattern was measured by a diffraction counter method using a position-sensitive proportional counter system. A sample was packed into a glass capillary and set in a high-temperature cell equipped with a temperature controller (fluctuation within $\pm 0.5^\circ\text{C}$). Polarized infra-red spectra of the samples obtained before and after poling were measured at room temperature by a JASCO A-III infra-red spectrophotometer.

RESULTS AND DISCUSSION

X-ray pattern change induced by poling

In Figure 2 are shown the X-ray photographs of VDF 52% copolymer taken for the low-temperature phase (Figure 2a), the cooled phase (Figure 2b), and the sample obtained by poling the cooled phase (Figures 2c and 2d). In Figure 2c the incident X-ray beams are parallel to the electric field E or normal to the film surface, and in Figure 2d they are perpendicular to E . The characteristic features in the X-ray diffraction pattern of the cooled phase are the tilting phenomenon and the broadness of reflections as

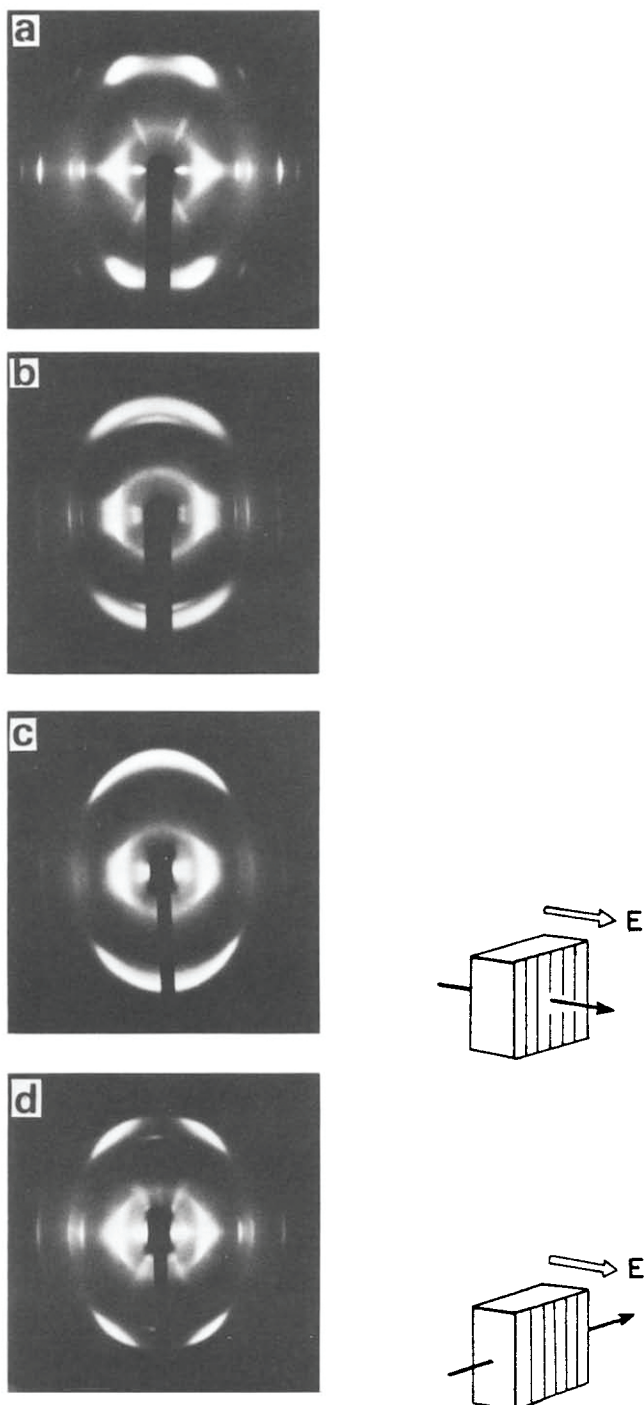


Figure 2 X-ray photographs taken for the various crystalline states of VDF 52% copolymer: (a) the low-temperature phase, (b) the cooled phase, (c) and (d) the poled sample. The draw direction is vertical

pointed out above². The tilting of the chain axis from the draw direction shifts the position of X-ray reflectional spots upwards or downwards from the original horizontal lines, as shown in *Figure 2b*. In the low-temperature phase, which is prepared by stretching the cooled phase along the draw axis, the tilting phenomenon disappears almost completely and the layer-line reflections are remarkably sharp as seen in *Figure 2a*. In the uniaxially oriented samples of *Figures 2a* and *2b*, almost no anisotropy in the X-ray pattern is detected for any scattering geometry of X-ray beams incident along the direction perpendicular to the draw axis. But in the poling-treated sample, the X-ray patterns are much

different between the two scattering geometries, as shown in *Figures 2c* and *2d*. Such an anisotropy can be seen typically in the relative intensities of the equatorial reflections and also in the whole pattern of a group of (201, 1 1 1) reflections in the first layer line. The reflections are considerably sharp compared with those of the cooled phase and the estimated unit-cell dimensions are $a=9.12 \text{ \AA}$, $b=5.22 \text{ \AA}$, c (fibre axis) $=2.55 \text{ \AA}$ and $\beta=93^\circ$, coincident with those of the low-temperature phase ($a=9.12 \text{ \AA}$, $b=5.25 \text{ \AA}$, $c=2.55 \text{ \AA}$ and $\beta=93^\circ$)². Thus it may be considered that the high electric field transforms the disordered cooled phase to the regular low-temperature phase. Although such a phase transformation is just like the case of tensile stress, tilting can still be detected in the poling sample and the tilting direction and angle remain unchanged after poling. Additionally, as seen in *Figures 2c* and *2d* (and also in *Figure 6*), the (001) reflection is observed on the meridional line for X-ray beam perpendicular to E but not for X-ray beam parallel to E , indicating that the tilting phenomenon occurs in a particular direction of the film sample. The details will be discussed later.

As pointed out above, the X-ray intensities of equatorial reflections are also different for the two cases of diffraction geometry (*Figures 2c* and *2d*). In *Figure 3* is shown the dependence of the (020) reflection intensity upon the angle ϕ , which is defined as shown in the inset. In *Figure 4* the relative peak intensity of this reflection is plotted against ϕ . From these figures we may say that there is almost no preferential orientation of the crystallites around the draw axis in the cooled phase. In contrast, for the poled sample, the (020) reflection has an intensity maximum at $\phi=0^\circ$, indicating that the b axis orients preferentially into the direction normal to the film plane, i.e. into the direction of the applied electric field. Such a dipole reorientation can be detected also in the polarized infra-red spectra. As shown in *Figure 5*, the perpendicular component of CH_2 symmetric stretching band $\nu_s(\text{CH}_2)$ decreases in intensity and that of CH_2 antisymmetric stretching band $\nu_a(\text{CH}_2)$ increases after poling. The infra-red absorption intensity is proportional to the scalar product of the transition dipole moment and the electric field vector of the incident infra-red beam. The transition moments of $\nu_s(\text{CH}_2)$ and $\nu_a(\text{CH}_2)$ are approximately parallel and perpendicular to the b axis, respectively, and the electric field vector of the incident infra-red beam is within the film plane. Thus the intensity change in *Figure 5* indicates that the b axis reorients in the direction of the poling electric field^{12,13}.

For the VDF 65% sample, in contrast to the case of VDF 52%, the initial sample obtained by cooling the high-temperature phase is a mixture of the low-temperature and the cooled phases, both showing the tilting phenomenon. When it is poled under a high electric field, the X-ray photograph of the low-temperature phase is like that obtained for VDF 52% (see *Figure 6*). The whole pattern and relative intensity of reflections are different between the two cases of incident X-ray beams parallel and perpendicular to E . Chain tilting is still observed and the direction and angle are also unchanged even after poling.

In this way poling of the cooled samples of VDF 52% and 65% copolymers transfers the disordered phase into the ordered one with the b axis reoriented parallel to the electric field (*Figure 7*), just when the tilting phenomenon

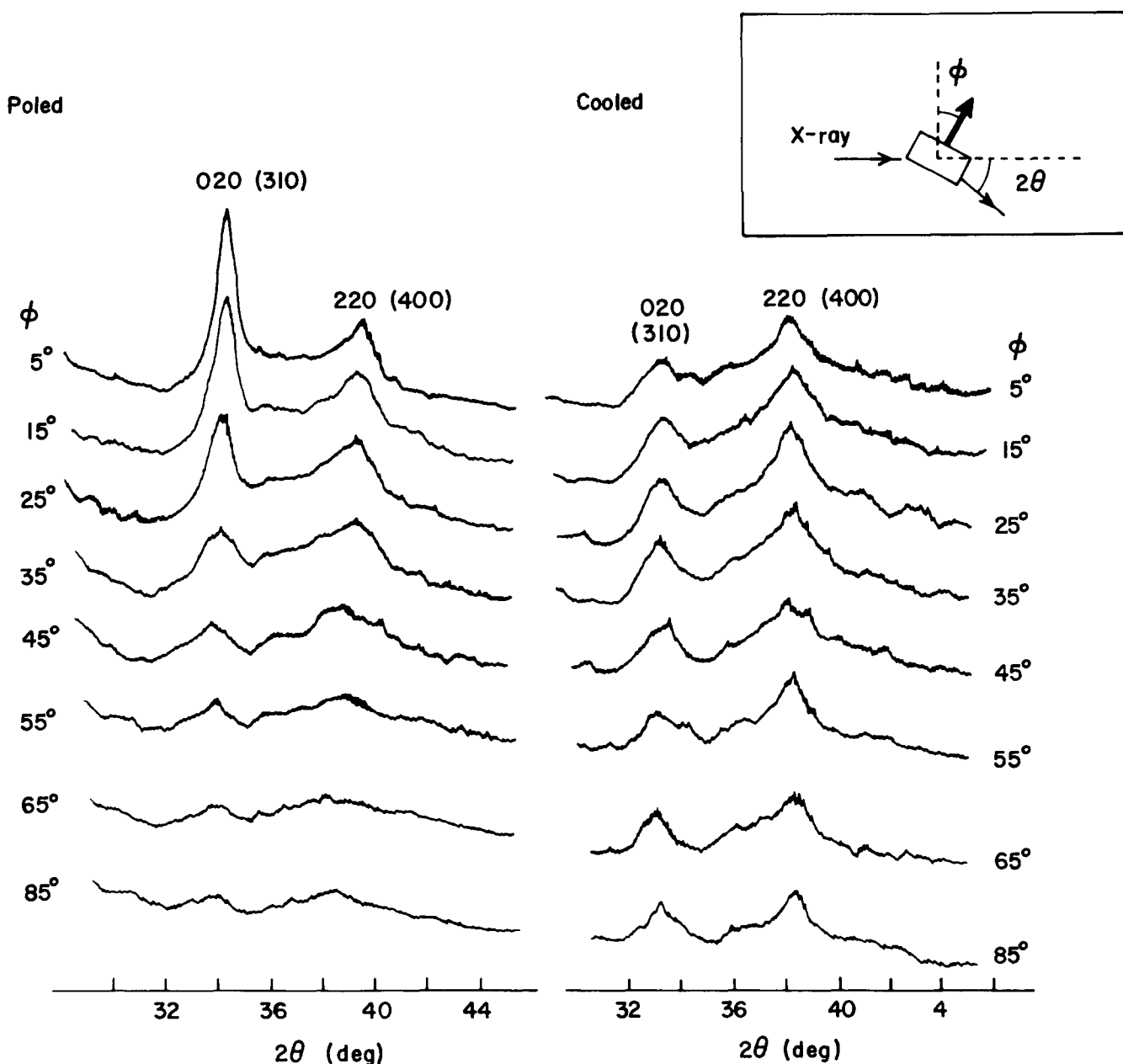


Figure 3 Dependence of X-ray reflections of VDF 52% copolymer on the angle ϕ (defined in the inset). Based on the calculation of structure factor, the main reciprocal lattice points contributing to these reflections are 020 and 220, although the other reciprocal points shown in parentheses also contribute more or less

of the zigzag chains are still reserved. By taking these structural features into consideration, we calculated the position of reflections on the X-ray photograph predicted for the poled samples. An example of the VDF 65% case is illustrated in Figure 6, where the unit-cell parameters are as follows: $a=8.92 \text{ \AA}$, $b=5.17 \text{ \AA}$, $c=2.55 \text{ \AA}$, $\beta=93^\circ$, tilting plane=(130), and tilting angle= 18° . The calculated reflectional positions (full circles) correspond well to the observed ones for both cases of X-ray beam perpendicular and parallel to E . In Figure 8 is shown a model in which the *trans* zigzag chain tilts by 18° in the (130) plane and the b axis or CF_2 dipoles orient to the direction of the electric field; Figure 8a is a view along the electric field or the y axis and Figure 8b is a view normal to the field or along the x axis. From this figure we can notice easily that the zigzag chain inclines approximately within the xz or ac plane. Corresponding to such a chain tilting in real space, the c^* axis tilts preferentially within the (a^*c^*)

plane in reciprocal space. (As shown in Figure 9, the c^* axis tilts from the elongation axis around the tilt line $\{130\}$, but to a good approximation this tilt line may be assumed to be the b^* axis.) Such preferential tilting of the c^* axis is a reason why the (001) reflection could be observed in Figures 2 and 6 only for the case of the incident X-ray beams perpendicular to the electric field; that is to say, the (001) reciprocal lattice point can contact with the so-called Ewald sphere, the necessary condition for an occurrence of X-ray reflection¹⁴, only for the above case but not for the case of the X-ray beams parallel to E .

Additional information from Weissenberg photographs

Although the cylindrical X-ray photographs of Figures 2 and 6 indicate clearly the existence of chain tilting as discussed above, the Weissenberg photograph suggests that the poled sample must also contain the crystalline chains that stand vertically along the draw axis in

addition to the tilted chains. In Figure 10 are shown the Weissenberg photographs of VDF 65% copolymer developed for the $(00l)$ reflections by Norman's method¹⁴. In the cooled phase the (001) and (002) reflections split into two points from the central line corresponding to the draw axis because of the tilting phenomenon of the chains. But, for the poled sample, these reflections are observed in a different fashion for the two scattering geometries: for the X-ray beam perpendicular to the electric field the (001) and (002) reflections appear as a long arc, while for the X-ray beam parallel to the electric field spot-like reflections appear on the line corresponding to the draw axis. In the reciprocal

space of Figure 11 (refer to Figure 9), we consider overlap of two orientation states of the c^* axis: (1) the c^* axis tilts by about 18° from the draw axis around the tilt line of $\{130\}$ or approximately within the (a^*c^*) plane, and (2) the c^* axis is parallel to the draw axis. When the Weissenberg photograph is taken with the sample rotated around the a^* axis and with the X-ray beam incident along the b^* axis, only one reciprocal point among the three possible $(00l)$'s can cross the Ewald sphere and so only one reflection is observed on the photograph (see Figure 11a(i)). When the sample is rotated round the b^* axis and the X-ray beam is parallel to the a^* axis, three $(00l)$ points can cross the Ewald sphere with a constant

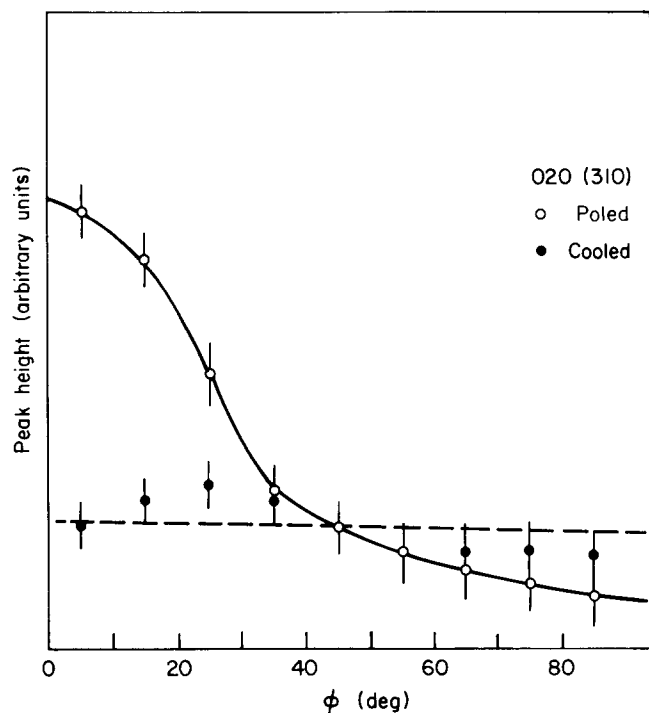


Figure 4 Angle ϕ dependence of X-ray intensity of the low-temperature reflection $(0\ 2\ 0)$. The definition of angle ϕ is given in Figure 3

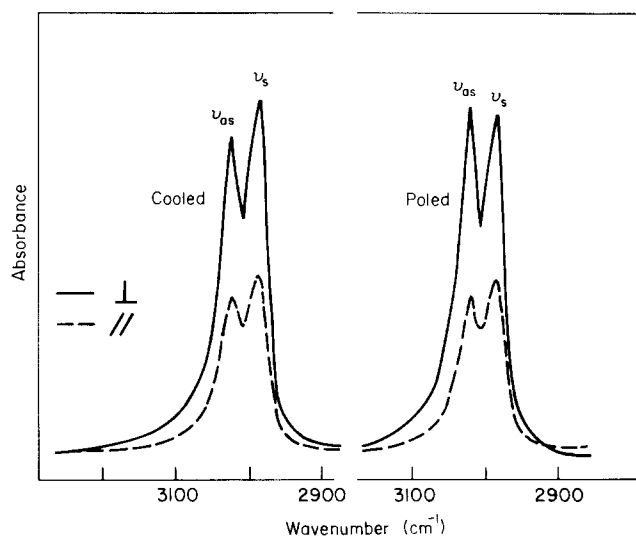


Figure 5 Polarized infra-red spectra of VDF 52% copolymer taken before and after poling in the frequency region $2900\text{--}3200\text{ cm}^{-1}$. ν_s and ν_{as} denote the symmetric and antisymmetric stretching modes of the CH_2 group, respectively. The full curve is for the electric vector of the incident infra-red beam perpendicular to the orientation axis; the broken curve is for the electric vector of the incident infra-red beam parallel to the orientation axis

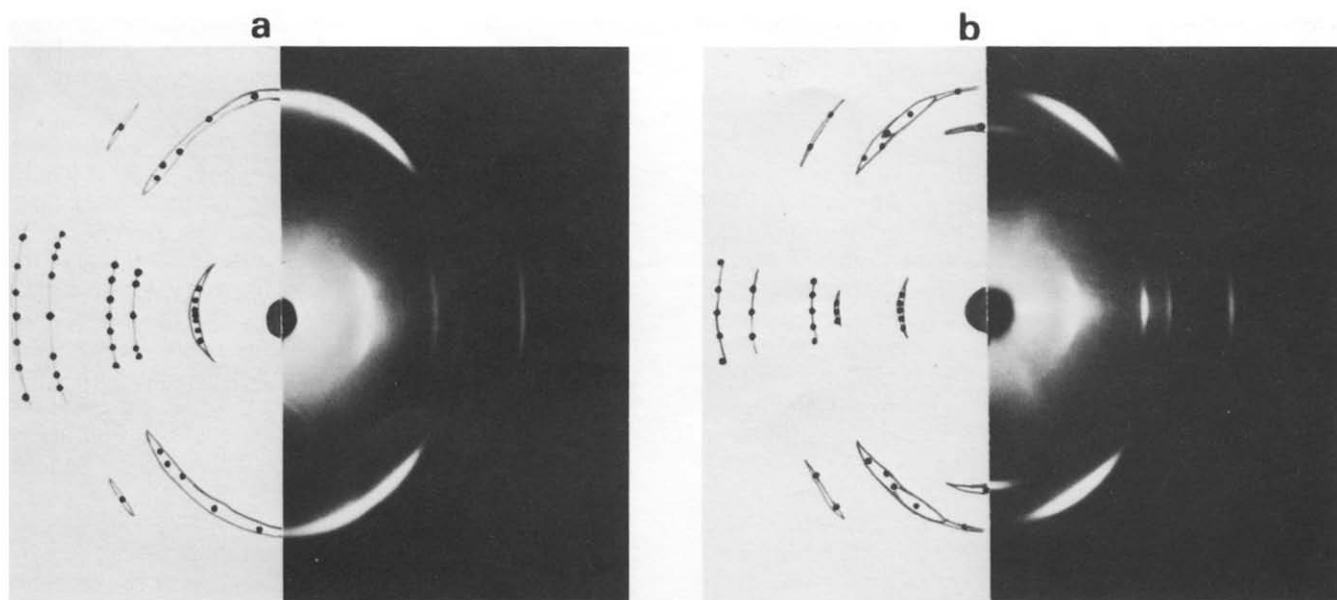


Figure 6 X-ray photographs of the poled VDF 65% sample taken with the incident X-ray beam (a) parallel, and (b) perpendicular to the electric field E . The left-hand side of each figure shows the reflection spots calculated by taking into account both the tilting and untilting phenomena of the zigzag chains by an angle 18° in the $(1\ 3\ 0)$ plane

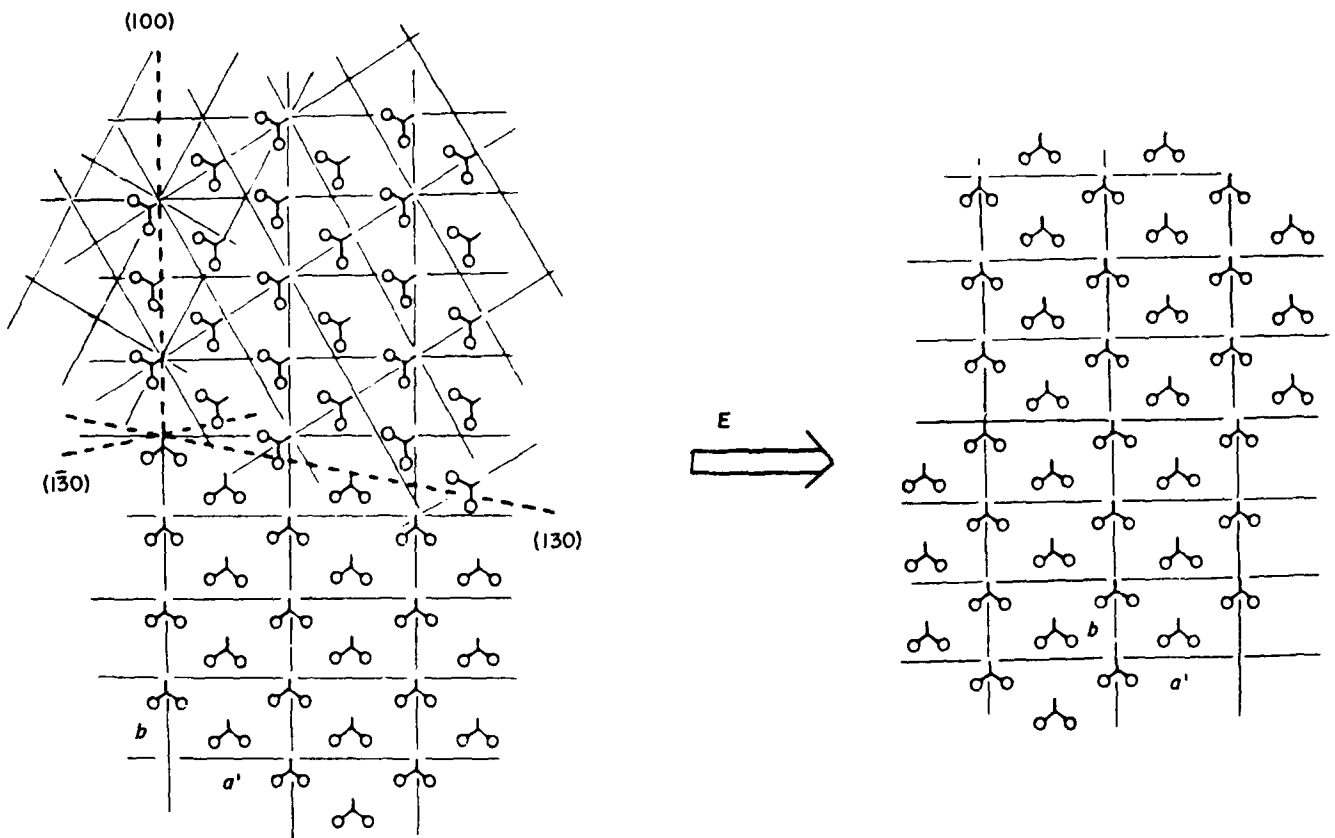


Figure 7 An illustration of dipole reorientation induced by the poling of the cooled phase. The (100), (130) and (130) planes are domain walls between the different dipole orientations

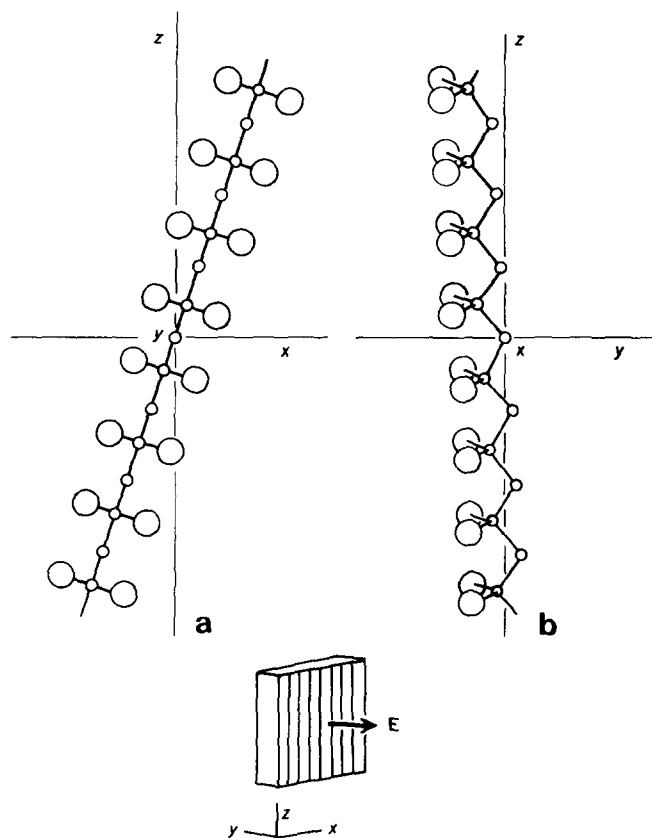


Figure 8 An illustration of the tilting of an all-trans chain segment within the (130) plane by an angle 18°

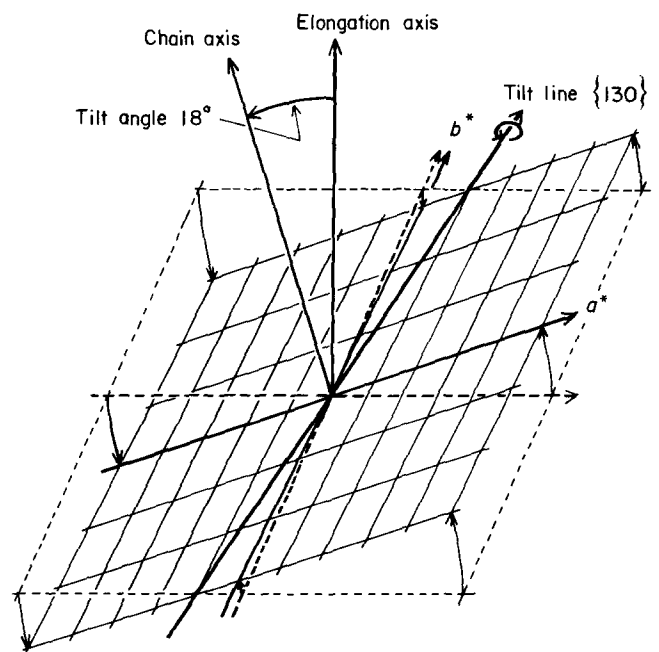


Figure 9 Tilting phenomenon in the reciprocal lattice (equatorial plane) of the VDF-TrFE copolymer

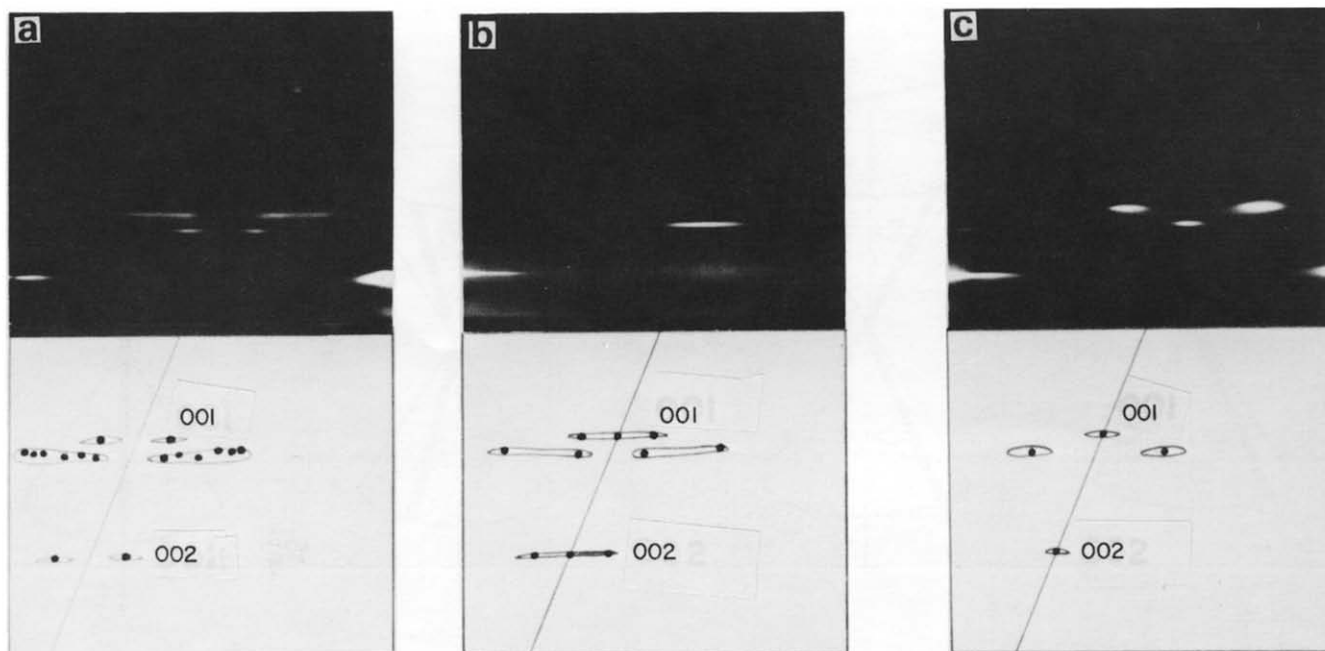


Figure 10 Weissenberg photographs taken by Norman's method for the VDF 65% copolymer oriented samples: (a) the cooled phase, (b) the poled sample with incident X-ray beam perpendicular to the electric field and (c) the poled sample with the incident X-ray beam parallel to the electric field. The full circles in the lower half of the figures represent the reflectional positions calculated by taking into account the tilting phenomenon. The central straight lines correspond to the draw axis of the oriented samples. It should be noted that in the photographs of the poled sample there exists a strong anisotropy of relative intensity for the (201) and (111) reflections located near the (001) reflection

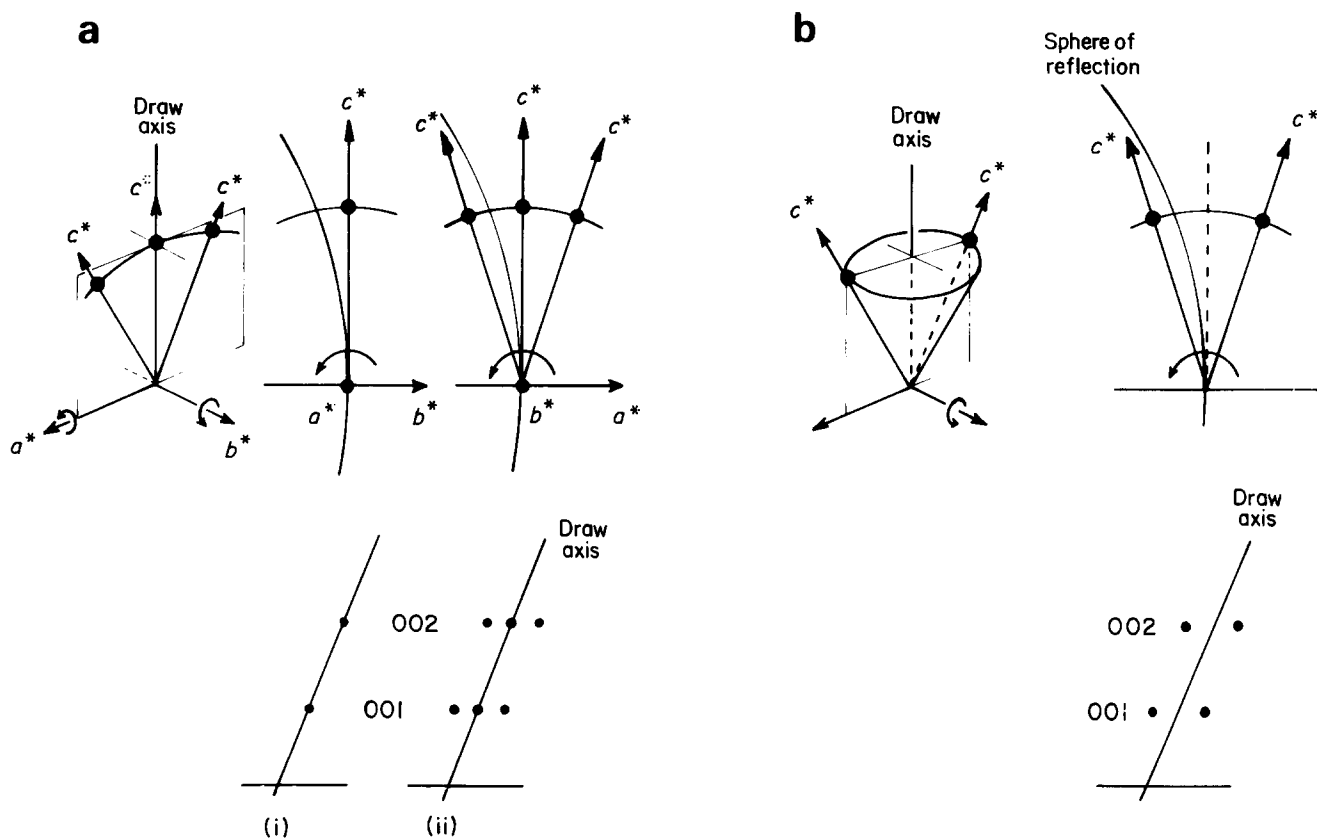


Figure 11 Illustrated explanation of the relationship between the reciprocal lattice points and the Weissenberg photograph for the meridional (001) and (002) reflections: (a) the poled sample and (b) the cooled phase

time interval. Since in the Weissenberg measurement the X-ray film is translated horizontally with time, three separated points can be observed on the photograph as a result. But, taking into account the effect of incomplete orientation in the draw film and the broadness of reflections, these three spots are smeared into one continuous and long arc in the actual photograph, as

shown in *Figure 10*. *Figure 11b* shows the case of the cooled phase, which should be compared with the photograph of *Figure 10a*.

A model for structural change induced by poling

As stated above, the crystallites orient almost homogeneously around the draw axis in the sample of the

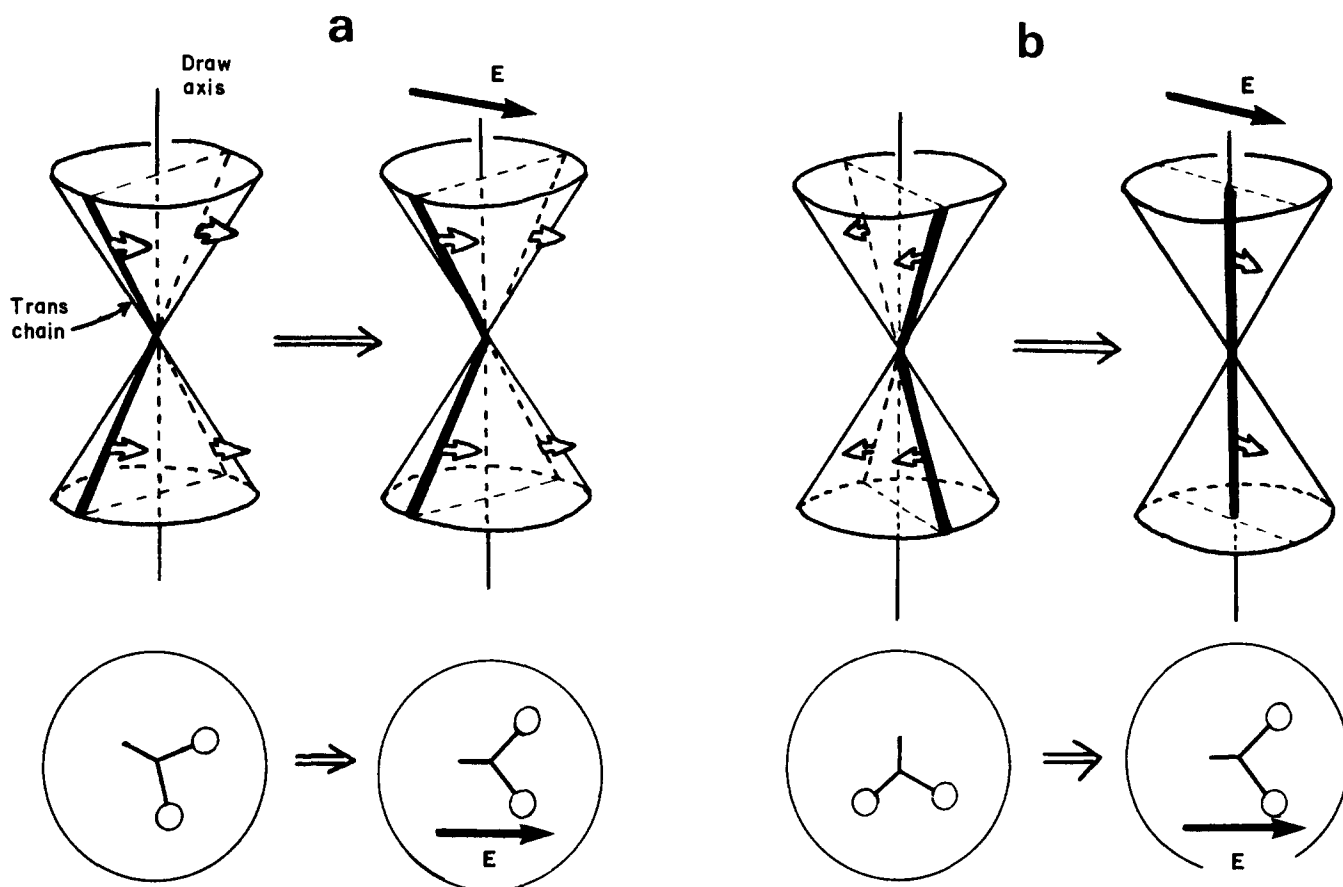


Figure 12 A model for the structural change in the cooled phase induced by an external electric field. The bold lines represent the *trans* zigzag segments with the dipoles denoted by arrows. The circular cones represent the distribution of tilted *trans* chains around the draw axis

cooled phase. When the high electric field is applied to this sample, each crystallite may react to the field in a different manner. For example, in a crystallite with dipole closely parallel to the applied electric field, the dipole reorientation into the direction of the applied electric field may occur easily while keeping the tilting character unchanged (see *Figure 12a*). On the other hand, in a crystallite where the CF_2 dipoles of the zigzag chains are arrayed almost perpendicular to the electric field, the tilted segments may rise up vertically as the dipole reorientation is induced by the electric field (see *Figure 12b*). An overlapping of these two different crystalline states may give the complicated Weissenberg photographs as discussed above. This is an extremely simplified model and there might also exist a crystallite of intermediate situation between that in *Figures 12a* and *12b*. But it may be reasonable to consider that an essential structural feature of the poled sample can be described using the present model. When the dipoles are reoriented towards the electric field, it may be impossible to rotate the whole chain segment rigidly. It is plausible to assume a mechanism in which a soliton-like motion along the chain direction of some defect (for example, a skew or *gauche* linkage connecting neighbouring *trans* segments shown in *Figure 1*) induces a gradual rotation of neighbouring CF_2 dipoles into the electric field. Such a reorientation mechanism of CF_2 dipoles has already been pointed out for PVDF form I by Hopfinger *et al.*^{15,16}

Influence of poling on the phase transitional behaviour

Ordering in crystal structure caused by poling reflects on the halfwidth of X-ray reflections. As shown in *Table 1*,

Table 1 Integrated halfwidth of the X-ray reflections for the VDF 52% and 65% copolymer samples (in 10^{-2} rad)^a

	Reflection	Cooled	Poled	Low-temperature
VDF 65%	(001)	1.43	0.94	1.06
	(002)	1.89	1.26	1.30
	(200, 110)	1.70	1.20	0.84
VDF 52%	(001)	3.46	1.67	1.06
	(002)	6.45	2.38	1.39

^a No correction is made for the slit width

the integrated halfwidth of the equatorial and meridional reflections becomes sharper by poling the cooled phase and furthermore sharper by drawing the cooled phase. Such a tendency is detected more clearly for the VDF 52% copolymer than for the VDF 65% sample (the accuracy of the estimated halfwidth is within about $\pm 0.05 \times 10^{-2}$ rad). As reported in previous papers^{2,3}, the low-temperature phase transforms to the paraelectric high-temperature phase at higher temperature than is the case for the cooled phase. Then, referring to the result of *Table 1*, it may be expected that the structural ordering induced by poling also shifts the transition point to higher temperature. In fact, Lovinger *et al.*^{10,11} found such a temperature shift for unoriented but poled samples. We have studied such a poling effect on the transitional behaviour in more detail.

Figure 13 shows the temperature dependence of X-ray (200, 110) reflection for the VDF 65% sample. *Figure 13a* is for the sample of the low-temperature phase. The reflection of the high-temperature phase does not appear below 90°C but it begins to appear rapidly with increasing

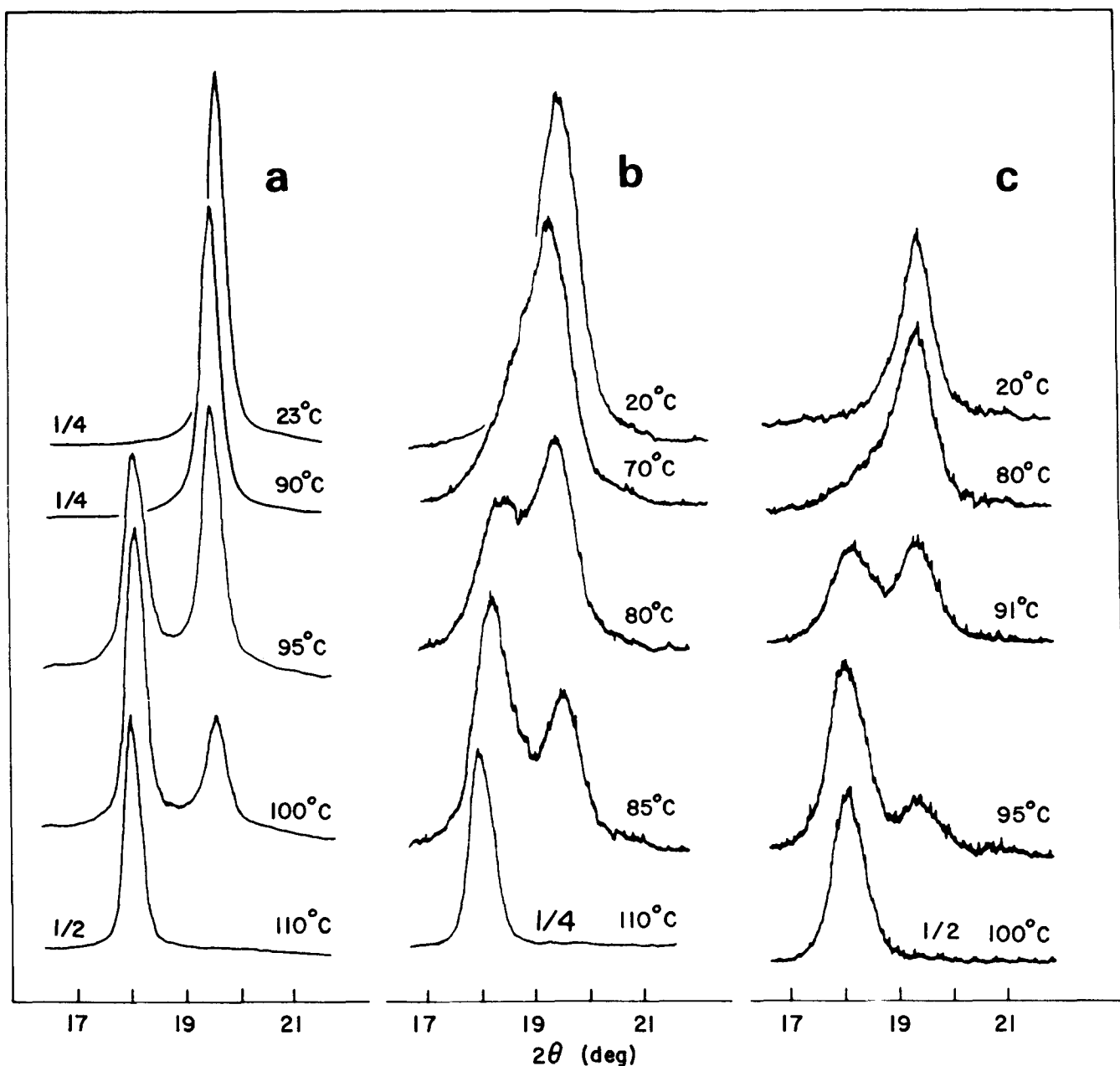


Figure 13 Temperature dependence of the X-ray (200, 110) reflection profiles of VDF 65% copolymers: (a) the low-temperature restretched phase, (b) the cooled phase and (c) the poled sample of (b) with incident X-ray beam parallel to the electric field

temperature only a little above 90°C. In *Figure 14a* is plotted the relative intensity of the low-temperature phase against the temperature. In the cooled phase (*Figure 13b*), the transition is rather broad and the X-ray reflection of the high-temperature phase can be detected even near 75°C. Such transitional behaviour of the cooled phase does not depend so strongly on whether the cooled phase is oriented or unoriented as understood in *Figures 14c* and *14d*. In the poled sample (*Figure 13c*), the transition becomes considerably sharp compared with the case of the cooled phase, and the transition point shifts towards that of the low-temperature phase (*Figure 13a*). In the cooling process from the high-temperature phase, all the samples transform to the cooled phase (more strictly speaking, to the mixture of the low-temperature and cooled phases in the VDF 65% case) and the behaviour is essentially equivalent to each other.

In this way the phase transition becomes sharper and the transition point shifts to higher temperature by poling

of the cooled phase. The observation of this transitional temperature shift is consistent with Lovinger's report^{10,11}. They stated that there is only a slight effect of drawing on the transitional behaviour of VDF 65% sample. But their sample is possibly considered to correspond to the cooled phase, as seen in *Figures 14c* and *14d*. We must note that the sample of *Figure 14a*, the low-temperature phase, which is prepared by elongating further the oriented cooled phase at room temperature and gives a very good X-ray pattern, exhibits a very sharp phase transition at a higher temperature. That is to say, we can recognize not only a poling effect but also a remarkable elongation effect on the transitional behaviour.

CONCLUSIONS

In the present paper we describe the transformation from disordered to ordered crystal structure by applying a

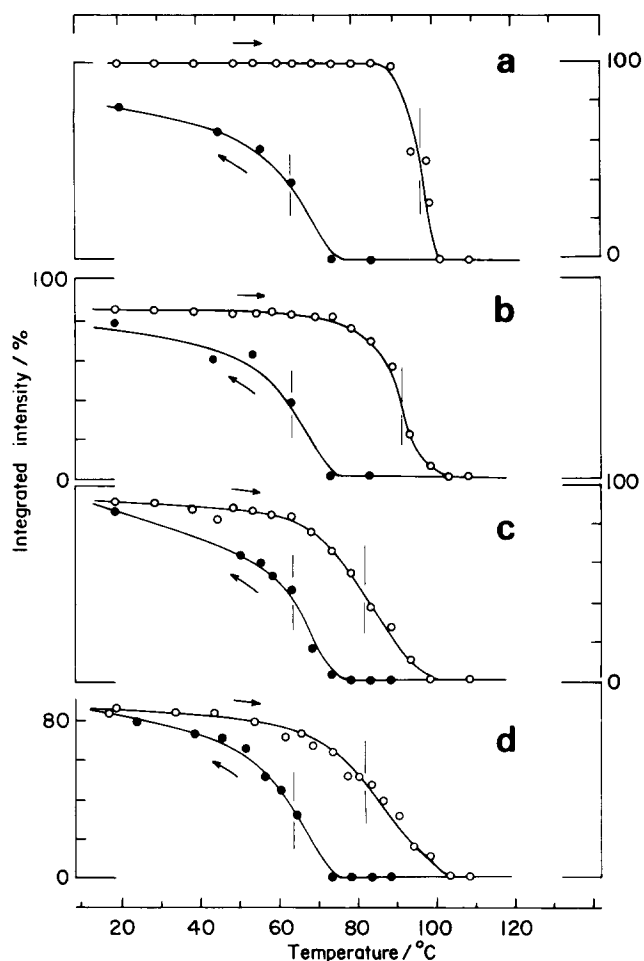


Figure 14 Temperature dependence of integrated intensity of the low-temperature (200, 110) reflection for the VDF 65% samples: (a) the oriented low-temperature phase, (b) the oriented sample obtained by poling the cooled phase, (c) the oriented cooled phase and (d) the unoriented cooled phase

tensile stress or a high electric field to the cooled phase. The effects of these two external fields are appreciably different from each other. In the elongation process the tilting phenomenon of the cooled phase disappears and the well oriented and highly regular low-temperature phase is obtained. In the poling process some fraction of the crystallites transform to the low-temperature phase while holding the tilting character of the zigzag chains and another fraction of the crystallites transform to the nontilted low-temperature phase. Simultaneously we can recognize the reorientation process of *trans* zigzag dipoles into the direction of the applied electric field. The transition mechanism is considered to be quite

complicated, as discussed in the previous section. The phase transitional behaviour is also affected by such a poling process and the sharper structural change from *trans* to *gauche* phases is observed at higher temperature compared with the case of the unpoled cooled phase. The transitional temperature shift can be ascribed to ordering in the crystal structure and is also detected for the case of elongation of the oriented cooled phase into the low-temperature phase.

ACKNOWLEDGEMENTS

The authors are grateful to Drs Syun Koizumi, Junichi Sako, Toshiharu Yagi and Yoshihide Higashihata of Daikin Kogyo Co. Ltd in Japan for supplying samples of VDF-TrFE copolymers. They wish also to thank Emeritus Professor Hiroyuki Tadokoro of Osaka University for his continuous encouragement. This work was supported in part by a Grant-in-Aid on Special Project Research for 'Organic Thin Films for Information Conversion' from the Ministry of Education, Science, and Culture of Japan.

REFERENCES

- 1 Tashiro, K., Takano, K., Kobayashi, M., Chatani, Y. and Tadokoro, H. *Polymer* 1981, **22**, 1312
- 2 Tashiro, K., Takano, K., Kobayashi, M., Chatani, Y. and Tadokoro, H. *Polymer* 1984, **25**, 195
- 3 Tashiro, K., Takano, K., Kobayashi, M., Chatani, Y. and Tadokoro, H. *Ferroelectrics* 1984, **57**, 297
- 4 Tashiro, K., Nakamura, M., Kobayashi, M., Chatani, Y. and Tadokoro, H. *Macromolecules* 1984, **17**, 1452
- 5 Odajima, A. and Tashiro, K. *J. Crystallogr. Soc. Jpn.* 1984, **26**, 103
- 6 Hasegawa, R., Takahashi, Y., Chatani, Y. and Tadokoro, H. *Polym. J.* 1972, **3**, 600
- 7 Daubeny, R. de P., Bunn, C. W. and Brown, C. J. *Proc. R. Soc. A* 1954, **226**, 531
- 8 Lovinger, A. J., Davis, G. T., Furukawa, T. and Broadhurst, M. G. *Macromolecules* 1982, **15**, 323
- 9 Davis, G. T., Furukawa, T., Lovinger, A. J. and Broadhurst, M. G. *Macromolecules* 1982, **15**, 329
- 10 Lovinger, A. J., Furukawa, T., Davis, G. T. and Broadhurst, M. G. *Polymer* 1983, **24**, 1225
- 11 Lovinger, A. J., Furukawa, T., Davis, G. T. and Broadhurst, M. G. *Polymer* 1983, **24**, 1233
- 12 Naegele, D. and Yoon, D. Y. *Appl. Phys. Lett.* 1980, **37**, 791
- 13 Takahashi, T., Date, M. and Fukada, E. *Appl. Phys. Lett.* 1980, **37**, 791
- 14 Tadokoro, H. 'Structure of Crystalline Polymers', John Wiley, New York, 1979
- 15 Dvey-Aharon, H., Sluckin, T. J., Taylor, P. L. and Hopfinger, A. J. *Phys. Rev. B* 1980, **21**, 3700
- 16 Hopfinger, A. J., Lewanski, A. J., Sluckin, T. J. and Taylor, P. L. *Springer Ser. Solid-State Sci.* 1978, **8**, 334